

Quantum melting on a lattice and a delocalization transition

E. V. Tsiper,¹ F. G. Pikus,² A. L. Efros¹

¹ *Department of Physics, University of Utah, Salt Lake City, UT 84112*

² *Department of Physics, University of California at Santa Barbara, Santa Barbara, CA 93106*

(November 14, 2016)

Abstract

We consider $2d$ gas of spinless fermions with the Coulomb interaction on a lattice at $T = 0$ and at different values of the hopping amplitude J . At small J electrons form a periodic structure. At filling factor $\nu = 1/6$ this structure melts at J as low as 0.02–0.03 in units of the nearest-neighbor Coulomb energy. We argue that this transition is connected to the dielectric-metal or dielectric-superconductor transitions. To demonstrate this point we perform computer modeling of the systems 6×6 with 6 and 7 electrons and 6×12 with 12 electrons. By sweeping J we compute simultaneously persistent current and structural characteristics of the electron distribution.

71.30.+h,73.20.Jc,61.20.Ja

arXiv:cond-mat/9512150v2 7 Mar 1996

The great majority of the efforts made recently to study correlated particles on a lattice were restricted to the Hubbard model or $t - J$ model (See review [1]). We concentrate here on a direct interaction between particles which introduces some important new physical features. We consider spinless fermions at $T = 0$ on a 2-dimensional square lattice with the following Hamiltonian

$$H = J \sum_{\mathbf{r}, \mathbf{s}} a_{\mathbf{r}+\mathbf{s}}^\dagger a_{\mathbf{r}} \exp(i\boldsymbol{\phi}\mathbf{s}) + \frac{1}{2} \sum_{\mathbf{r} \neq \mathbf{r}'} \frac{n_{\mathbf{r}} n_{\mathbf{r}'}}{|\mathbf{r} - \mathbf{r}'|}. \quad (1)$$

Here $n_{\mathbf{r}} = a_{\mathbf{r}}^\dagger a_{\mathbf{r}}$, the summation is performed over the lattice sites \mathbf{r} , \mathbf{r}' and over the vectors of translations to the nearest-neighbor sites, \mathbf{s} . The lattice constant and the Coulomb energy between nearest neighbors are chosen to be the length and energy units. We use periodic conditions at the boundaries of rectangle $L_x \times L_y$. The dimensionless vector potential $\boldsymbol{\phi} = (\phi_x, \phi_y)$ in the Hamiltonian is equivalent to the twist of the boundary conditions by the flux $\Phi_i = L_i \phi_i$, $i = x, y$. The total spectrum is periodic in Φ_x and Φ_y with the period 2π .

In a commensurate phase, at small enough values of J , fermions form a Wigner crystal (WC) with the long range order. At $T = 0$ and some critical value J_c the crystal melts. Not much is known about the quantum melting on a lattice. The only exactly solvable model [2] is a 1-d model with the nearest-neighbor interaction and with the filling factor $\nu = 1/2$.

In 2-d case a computer modeling made by Pikus and Efros [3] at $\nu = 1/3$ and $1/6$ in a square 6×6 shows that J_c is as low as 0.03–0.02. They argue that the lifting of degeneracy of the ground state is the best diagnostic of the transition. At $J = 0$ this is an exact degeneracy corresponding to the different translational positions of a crystal on a background lattice. In a finite array it is lifted at any small J but the splitting is proportional to $\exp(-N|\ln J|)$, where N is the total number of the particles. Above J_c one should expect a macroscopic splitting.

Since the Hamiltonian (1) is translationally invariant, the states of the system can be classified in terms of the total quasimomentum \mathbf{P} . The degeneracy of the ground state at $J < J_c$ means that the energy of the macroscopic system is independent of \mathbf{P} .

We show here that the structural transition is accompanied not only by the \mathbf{P} -splitting of

the ground state. It includes also a *delocalization*, defined as an appearance of the *persistent current*, i. e. dependence of the energy on the flux Φ . We have found that at small J the system is dielectric and at $J \approx J_c$ it comes to a new state, which can be either metallic or superconducting.

The WC in a continuous media without any disorder has the same flux response as free electrons [4]. The dielectric behavior of the lattice WC at small J can be understood in terms of the umklapp processes. Yet another explanation is also possible which resembles the ideas of Ref. [5]. Consider Hamiltonian Eq. (1) for two particles only. If the distance between the particles is such that their interaction energy is larger than the width of the band, which is $8J$, the particles form a bound state. They cannot be separated because of the energy conservation law. The center-of-mass motion for these two particles is allowed, but corresponding band has a width proportional to J^2 at small J . In the same way n interacting particles will also form a bound state with the bandwidth of the center-of-mass motion proportional to J^n . We may then conclude that a system of interacting particles blocks itself if an interaction energy at *average distance* is much larger than the width of the band. Note that this second interpretation is applicable not only to commensurate phases [6]. The transition we are considering is of a correlation nature. But it differs from the Mott-Hubbard transition because it occurs due to the interaction of remote electrons and because spin does not play any important role here.

As a basis for computations we use many-electron wave functions at $J = 0$. Their total number is C_M^N , where $M = L_x \times L_y$ is the area of a system. They can be visualized in a form of pictures, which we call *icons*. Some icons with the lowest energies are shown in Fig. 1. The lowest energy has the icon with a fragment of the crystal. Icons with larger energies may also represent periodic structures with a period less than the size of the system. The Coulomb energy has been calculated as a Madelung sum, assuming that the icons are repeated periodically through the infinite plane with a compensating homogeneous background. Each icon represents a Slater determinant Ψ_α .

For each icon α there are m_α different icons that can be obtained from it by various

translations. These icons are combined to get the wave function with total quasimomentum \mathbf{P} :

$$\Psi_{\alpha\mathbf{P}} = \frac{1}{\sqrt{m_\alpha}} \sum_{\mathbf{r}} \exp(i\mathbf{P}\mathbf{r}) T_{\mathbf{r}} \Psi_\alpha. \quad (2)$$

The summation is performed over m_α translations $T_{\mathbf{r}}$. Important point is that the icons with periodic structures generate smaller number of different functions $\Psi_{\alpha\mathbf{P}}$. The number of allowed \mathbf{P} generated by each icon is equal to m_α . In particular, for each icon of a WC with one electron per primitive cell, one has $m_0 = 1/\nu$.

The allowed values of \mathbf{P} generated by a WC icon are determined from the conditions $(-1)^{Q_j} \exp(i\mathbf{P}\mathbf{l}_j) = 1$. Here \mathbf{l}_j are the primitive vectors of the WC, and Q_j are the numbers of fermionic transmutations necessary for translations on these vectors. These conditions can be easily understood. If translation on a vector \mathbf{l}_j is applied to Eq. (2), the right-hand side acquires a factor $(-1)^{Q_j}$, while for a function with given \mathbf{P} this factor must be equal to $\exp(i\mathbf{P}\mathbf{l}_j)$. If Q_j are even for both \mathbf{l}_j , the allowed \mathbf{P} form the reciprocal lattice of the WC. However, in the case when one or both of Q_j are odd, the lattice is shifted by π in the corresponding directions. In such case $\mathbf{P} = 0$ is forbidden. The set of m_α nontrivial values of \mathbf{P} is restricted to the first Brillouin zone of the background lattice. One WC is represented by a number of icons obtained from each other by the point-group transformations of the background lattice. The total number of allowed values of \mathbf{P} for the WC is the property of the WC and does not depend on the size and the shape of the system. Contrary, an icon representing a point defect in a WC generates all vectors \mathbf{P} ; their total number is M .

The following results can be obtained directly from the perturbation theory with respect to J : 1. The ground state and the lowest excited states have a common large down shift which is proportional to J^2 and to the total number of particles N . 2. The ground state splitting appears in the N -th order and it is proportional to J^N . 3. The flux dependence of the ground state for the flux in x -direction appears in the L_x -th order and it is proportional to J^{L_x} .

The transition we are studying occurs at such small values of J that classification of

states in terms of icons is still useful. At small J there is a gap in the spectrum since a finite energy is required to create a point defect in the WC. The states originating from the WC icon do not belong to the continuous spectrum since their number remains finite in a macroscopic system. The states originating from an icon with point defect in WC form a band.

One can imagine two different scenarios of the transition. The simplest one is the first-order phase transition. It occurs if the branch originated from the point-defect icon crosses the ground state at $J = J_c$. This may happen because the energy of the bottom of the point-defect band is going down with increasing J and can overcome the Coulomb energy of the point defect existing at $J = 0$. The crossing is possible if the defect branch has \mathbf{P} different from all vectors of the WC. Since point defect may have all \mathbf{P} , the excitation spectrum of the large system will become continuous at $J > J_c$. Then the new state should be a normal metal.

In the second scenario the ground state eigenvector originated from the WC icon has an avoided crossing with defect states of the same \mathbf{P} . The ground state obtains a large admixture of the defect states, loses the structural long range order and becomes delocalized in terms of the persistent current. However, the gap between the ground state and an excited state remains finite. This would be the second-order transition and the resulting state might be superconducting.

We have performed numerical diagonalization of the Hamiltonian for the system 6×6 with 6 and 7 electrons, and for the system 6×12 with 12. The exact-diagonalization results for the system with 6 electrons are shown in Figs. 2 and 3. For 12 electrons the complete basis consists of 1.5×10^{13} functions and the exact diagonalization is impossible. We performed diagonalization with a truncated basis as proposed in Ref. [3]. Two sets of 2.9×10^7 and of 5.8×10^7 different icons have been created by the classical Monte-Carlo with the temperatures of generation [3] $T_g = 0.020$ and 0.025 correspondingly. These sets make approximately 1.9×10^{-5} and 3.8×10^{-5} of the complete basis. For each \mathbf{P} the size of the matrix was 4×10^5 and 8×10^5 respectively. The flux sensitivities S calculated by

diagonalization of these matrices are shown in Fig. 3 by open and solid symbols. Except a small region at $J \approx 0.03$ there is no visible difference between the results.

For 7 electrons we are able to check how the computations with truncated bases converge to an exact result [6]. We obtained the following empiric rule: if one takes 2 truncated basic sets, one twice as large as the other, the difference in the results gives an upper boundary for the error for the largest set. This rule is applicable to the computation of the total energy as well as for *difference* in energy caused, say, by flux. It works when the relative error is small.

We think the picture we observe in a system with 6 electrons resembles the second scenario proposed above since the defect branch never crosses the ground state. Fig. 2 shows a few lowest energies at different momenta \mathbf{P} as a function of J at zero flux. At $J = 0$ we get the Coulomb energies of icons. The energy of the lowest icon is taken as zero. The second order perturbation theory shift is calculated using the energies of icons to be $-177J^2$, and it is subtracted from the total energy. The state with $\mathbf{P} = (0, \pi)$ is the lowest at $J < 0.02$. At larger J the lowest state has $\mathbf{P} = (\pi/3, \pi/3)$ and it also originates from the WC icon.

To study delocalization we compute a flux sensitivity $S(\Phi) = E(\Phi) - E(0)$, the difference between the ground state energies with and without flux Φ . To give more information we plot in Fig. 3 the energy difference for two above-mentioned values of \mathbf{P} for all J . Each of these curves represents $S(\Phi)$ in the region of J where the branch with corresponding \mathbf{P} is the ground state. Fig. 3 shows data for $\phi \parallel \mathbf{P}$ and $\phi \perp \mathbf{P}$, $\Phi_{x,y}$ either 0 or π . One can see a sharp increase of S with J for both values of \mathbf{P} and both directions of ϕ . In agreement with the perturbation theory it is proportional to J^6 at $J \leq 0.02$.

The interpretation of the results for 6×12 system is more ambiguous. As one can see from Fig. 1 (e)–(h), the low-energy part of the spectrum is created by three icons with close energies. The lowest one represents the WC. Two others can be classified neither as a crystal nor as a point defect. They represent rather interdomain boundaries in the WC. At $J \approx 0.004$ the branch with $\mathbf{P} = (0, \pi/3)$ originated from the second icon becomes the

ground state. Such \mathbf{P} is not allowed for the WC. Therefore, the situation resembles the first scenario leading to the phase transition of the first order. We think, however, that the small Coulomb gap between these icons, and, as a result, small J_c should be considered as an artifact of a small system. Since in a macroscopic system the energy of an interdomain boundary is proportional to the size of the system, such icons do not contribute to the lowest part of the energy spectrum. In smaller 6×6 system such a boundary does not even appear because of the periodic conditions.

That is why we study the states originated from the WC icon ignoring that none of them is the ground state. The lowest state has $\mathbf{P} = (0, \pi)$ as in the case of 6×6 system. The functions corresponding to the 3 lowest icons have a very small admixture of each other and can be studied separately. The flux sensitivity S of the lowest $\mathbf{P} = (0, \pi)$ branch is shown in Fig. 3 by open and solid circles. The sharp step-like increase in S is the result of a crossing of two such branches. By open and solid squares we also show S for the branch with the largest admixture of the WC icon having in mind that due to the above arguments this branch might become the ground state in a macroscopic system. Note again, that the same branch with $\mathbf{P} = (0, \pi)$ is the ground state of the 6×6 system.

For the same WC branch in the system 6×12 we have calculated the correlation function $G(\mathbf{r} - \mathbf{r}') = \langle n_{\mathbf{r}} n_{\mathbf{r}'} \rangle$. At very small J the function $G(\boldsymbol{\rho})$ is close to 1 at all vectors $\boldsymbol{\rho}$ of the WC and close to zero otherwise. To demonstrate melting we plot in Fig. 3 the difference in G for two equivalent WC vectors $(3,0)$ and $(0,6)$ as a function of J . The difference is taken to cancel J^2 -term, which is the same for all equivalent points and does not show the loss of the long range order. One can see that the structural transformation appears in the same range of J as the delocalization.

The dependence $S(\Phi)$ shown in Fig. 4 for both 6 and 12 electrons at $J = 0.04$. In the first case this is the difference of two ground state energies, in the second case this is the change of energy in the WC branch. In both cases we have found a very strong admixture of the second harmonic, which dominates for the system with 12 electrons. This means an admixture of defects with double charge and it gives another argument that the state after

transition might be superconducting. The admixture is strong in the region $0.02 < J < 0.04$ and it becomes less both with decreasing and increasing J .

The value of S after the transition increases linearly with J and is of the order of J . This result agrees with an estimate from the London equation which gives $S \sim \nu m^{-1} \sim \nu J$, where m is an electron mass. The large magnitude of S is a result of a gap in the spectrum. The most interesting question is whether this gap survives in a macroscopic sample. We think this may happen because the gap originates from the excitation energy of a defect, and all relevant characteristics such as the width of the defect band and the matrix element of avoiding crossing with the ground state should not have a strong size dependence.

Finally, we have shown that strong electron correlations create a dielectric state in 2d gas with a narrow band, and we have studied the collapse of this state with increasing band width. Our data for $\nu = 1/6$ are more in favor of the dielectric-superconductor than the dielectric-metal transition.

We are grateful for useful discussions to L. P. Gor'kov, D. Mattis, E. I. Rashba, B. Z. Spivak, and Bill Sutherland. The work is supported by QUEST of UCSB, subagreement KK3017 and by SDSC. F. G. P. acknowledges support by grant NSF DMR 9308011.

REFERENCES

- [1] E. Dagotto, Rev. Mod. Phys. **66**, 763 (1994).
- [2] J. des Cloizeaux, J. Math. Phys. **7**, 2136 (1966), B. S. Shastry, B. Sutherland, Phys. Rev. Lett. **65**, 243 (1990).
- [3] F. G. Pikus, A. L. Efros, Solid State Commun. **92**, 485 (1994), *ibid.* **96**, 183 (1995).
- [4] Krive I. V. *et al.* Physica Scripta T, **54**, 123 (1994).
- [5] Yu. Kagan, L. A. Maksimov, Sov. Phys. JETP **38**, 307 (1974).
- [6] Our data for system 6×6 with 7 electrons also show localization at small J . These data will be published elsewhere.

FIGURES

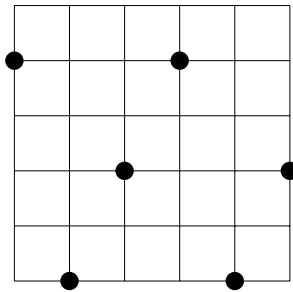
FIG. 1. Four icons with the lowest Coulomb energies for each of the two systems at $\nu = 1/6$. The total Coulomb energies E are shown above each icon. The lowest-energy icons (a,e) represent fragments of the same Wigner crystal.

FIG. 2. The low-energy part of the spectrum of the system 6×6 with 6 electrons as a function of J . The energy is measured from the Coulomb energy for the WC icon, $E_0 = -4.75547$. Branches with different quasimomentum \mathbf{P} are shown with different lines. The numbers in brackets show the components of the vector \mathbf{P} in units $\pi/3$.

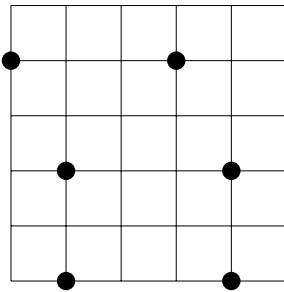
FIG. 3. Flux sensitivity $|S(\pi)|$ for different branches of the spectrum. The curves for the system 6×6 with 6 electrons are the result of exact diagonalization. The open and solid symbols show the results of diagonalizations of two truncated basic sets for the system 6×12 with 12 electrons. The sets I and II make approximately 1.9×10^{-5} and 3.8×10^{-5} of the complete basis. The diamonds show the difference in correlation function $G(\boldsymbol{\rho})$ for two equivalent WC vectors (3,0) and (0,6).

FIG. 4. Sensitivity $S(\Phi)$ as a function of Φ at $J = 0.04$ for two different systems. Note the strong admixture of the second harmonic, especially in the system 6×12 .

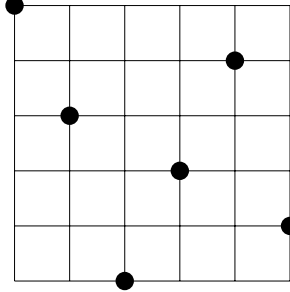
(a) $E = -4.75547$



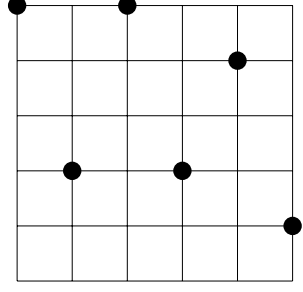
(b) $E = -4.71853$



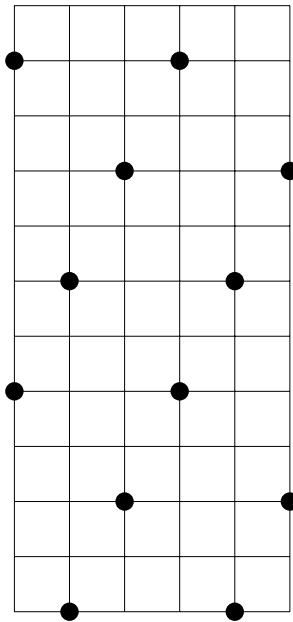
(c) $E = -4.71163$



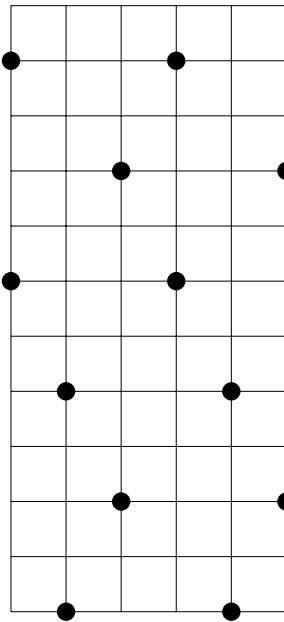
(d) $E = -4.67469$



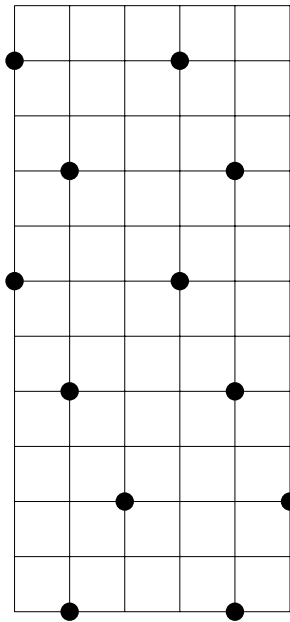
(e) $E = -9.51094$



(f) $E = -9.51018$



(g) $E = -9.50940$



(h) $E = -9.50862$

